High-efficiency multimode charging interface for Li-Ion battery with renewable energy sources in 180 nm CMOS

Hajjar Mamouni[1], Karim El Khadiri[2], Anass El Affar[3], Mohammed Ouazzani Jamil[4], Hassan Qjidaa[1]

[1]Department of Physics FSDM, Sidi Mohamed Ben Abdellah University Fez, Fez, Morocco
[2]Laboratory of Computer Science and Interdisciplinary Physics, ENS Sidi Mohamed Ben Abdellah University Fez, Fez, Morocco
[3]Laboratory of Engineering Sciences, Polydisciplinary Faculty in Taza Sidi Mohammed Ben Abdellah University of Fez, Fez, Morocco
[4]Faculty of Engineering Sciences, Private University of Fez, Fez, Morocco

Article Info

ABSTRACT

The high-efficiency multi-source Lithium-Ion battery charger with multiple renewable energy sources described in the present paper is based on supply voltage management and a variable current source. The goal of charging the battery in a constant current (CC) mode and controlling the supply voltage of the charging circuit are both made achievable using a variable current source, which may improve the battery charger's energy efficiency. The battery must be charged with a degraded current by switching from the CC state for the constant voltage (CV) state to prevent harming the Li-Ion battery. The Cadence Virtuoso simulator was utilized to obtain simulation results for the charging circuit, which is constructed in 0.18 μm CMOS technology. The simulation results obtained using the Cadence Virtuoso simulator, provide a holding current trickle charge (TC) of approximately 250 mA, a maximum charging current (LC) of approximately 1.3 A and a maximum battery voltage of 4.2 V, and takes only 29 minutes to charge.

Corresponding Author:

Hajjar Mamouni
Department of Physics FSDM, Sidi Mohamed Ben Abdellah University Fez
Fez, Morocco
Email: hajjar.mamouni@usmba.ac.ma

1. INTRODUCTION

Energy storage is a crucial process in the field of energy that involves conserving electricity generated during periods of surplus and releasing it when demand is high or when energy production is limited. Various energy storage technologies are used for this purpose, including batteries. To store energy from renewable sources, a variety of batteries are employed. The choice of battery depends on several factors, such as technology, storage capacity, lifespan, cost, and conditions of use. The long life, low self-discharge rate, and high energy density of Lithium-Ion batteries contribute to their increasing popularity [1]–[5]. They are used in many applications, including small- and large-scale renewable energy storage.

To date, several Lithium-Ion battery charger architectures have been developed using CMOS technology, among which is a charger based on a linear LDO regulator [6], [7]. The operating principle of this architecture uses a power transistor as a variable current source with two reference currents (Iref1 and Iref2) copied by a mirror to control the gate of the power transistor with a level shift. This setup generates a constant current (CC) that can vary between a holding current and a maximum current, allowing control of the three charging methods: trickle charge (TC), CC, and constant voltage (CV). However, due to the voltage discrepancy between the battery and the supply, this design suffers from a low energy efficiency rate, which fluctuates and increases the power dissipation of the active devices.

Another architecture is based on a buck and boost (DC-DC converter) [7]–[11]. This architecture is not well-suited for single-chip integration, as it has low accuracy despite its efficiency, large surface area requirements, and challenges with temperature control. In this article, we propose a multi-source charger that detects, sums, and manages two energy sources (photovoltaic and wind). The architecture of this invention is based on a non-inverting summing circuit that combines the two sources. This architecture includes two main blocks: the first is a power supply circuit based on a summing circuit. The purpose of this circuit is to obtain energy at all times, whether from the presence of wind or sun, the absence of one energy source (photovoltaic or wind), or when both are available but in limited amounts. This circuit sums the energy from the two sources to generate sufficient power to charge the Lithium-Ion battery. The second block is a circuit for charging the Lithium-Ion battery.

It relies on a variable current source, a charge controller that manages the three charge modes (TC, CC, and CV), and power supply management that maintains a small and steady differential between the power supply and battery voltage. The advantage of this charger is its high accuracy, increased energy efficiency, low power dissipation, and high integration. The proposed architecture optimizes energy transfer and improves system efficiency while ensuring better safety against battery overheating. This article is composed of five sections, the first one is the introduction, the overview of Lithium-Ion batteries in section 2, in the section 3 the proposed Lithium-Ion battery charger architecture and operating principal in section 4, the simulation result and discussions and the conclusion in the last section.

2.   OVERVIEW OF LI-ION BATTERIERS
2.1. Modelling for a Lithium-Ion battery
This model improves upon the simple version by incorporating an RC dipole, as shown in Figure 1 [12]. It consists of an ideal voltage source Voc, an internal resistor Rts, a capacitor representing the polarization of the battery's metal plates, and a surge resistor R due to the contact between the plates and the electrolyte. Although the elements of the circuit are often assumed to be constant, their values change in this model depending on temperature, discharge rate, and charge level. This model is known as the first-order Thévenin model [13], [14].
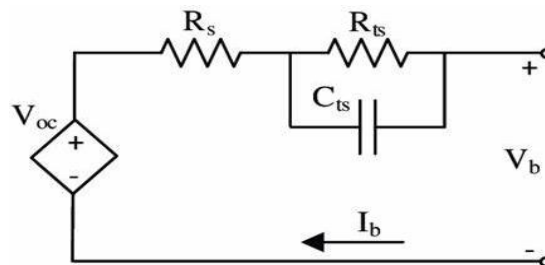
Figure 1. An equivalent Lithium-Ion battery circuit model

$$Uts = \frac{Uts}{C_{ts}\,R_{ts}} + I_p\frac{1}{C_{ts}} \tag{1}$$

$$V_b = V_{oc} - U_{ts} - R_s I_p \tag{2}$$

Uts: RC network voltage, also known as the battery polarization voltage.
R: Internal resistance of the battery.

2.2. The Lithium-Ion battery charging technique
The fundamental charging modes of a standard [15]–[19] Lithium-Ion battery are illustrated in Figure 2 shown following. The I_{BAT} battery current keeps going low when the V_{BAT} (battery voltage) falls below the V_{Low} voltage. This is done by using the TC charge mode, which guards against overheating and battery damage. Mode of charging with CC. In order to reduce the amount of time needed for charging when a battery's voltage falls between low and high (V_{Low} and V_{High}), a high, continuous current is provided to it [20]. When the VBAT battery voltage rises to the V_{High} high voltage standard value, which occurs in the CV charging mode, the IBAT battery current decreases to cut-off, ending the charging operation [21].
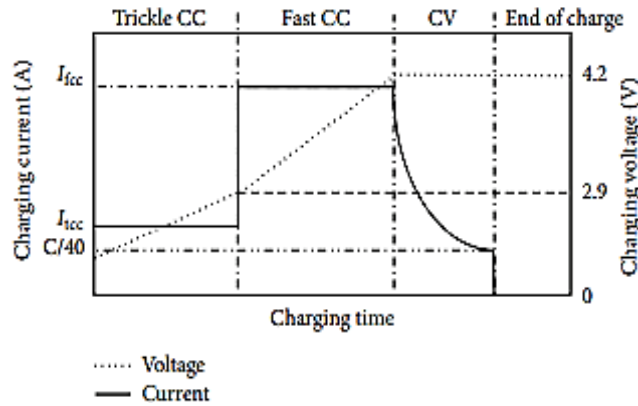
Figure 2. The method of charging Lithium-Ion batteries

3. PROPOSED LITHIUM-ION BATTERY CHARGER ARCHITECTURE AND OPERATING PRINCIPLE

The Figure 3 shows the proposed charging architecture and contains a power supply circuit that consists of a non-inverting analogue summing circuit for summing two renewable energy sources (photovoltaic and wind), which gives us a very accurate voltage, the charge mode controller that uses the reference current generator (RCG) to supply currents (I_{TC}, I_{LC}, and I_{CV}), There is a voltage block in the RCG.

The reference current for the CV charge mode is produced by the voltage block, and the reference currents for the CC charge mode and the end-of-charge current are produced by the current block. For every charge mode, a control voltage (V_C) is supplied by the charge current controller (CCC) from the current source to the current sensor circuit.
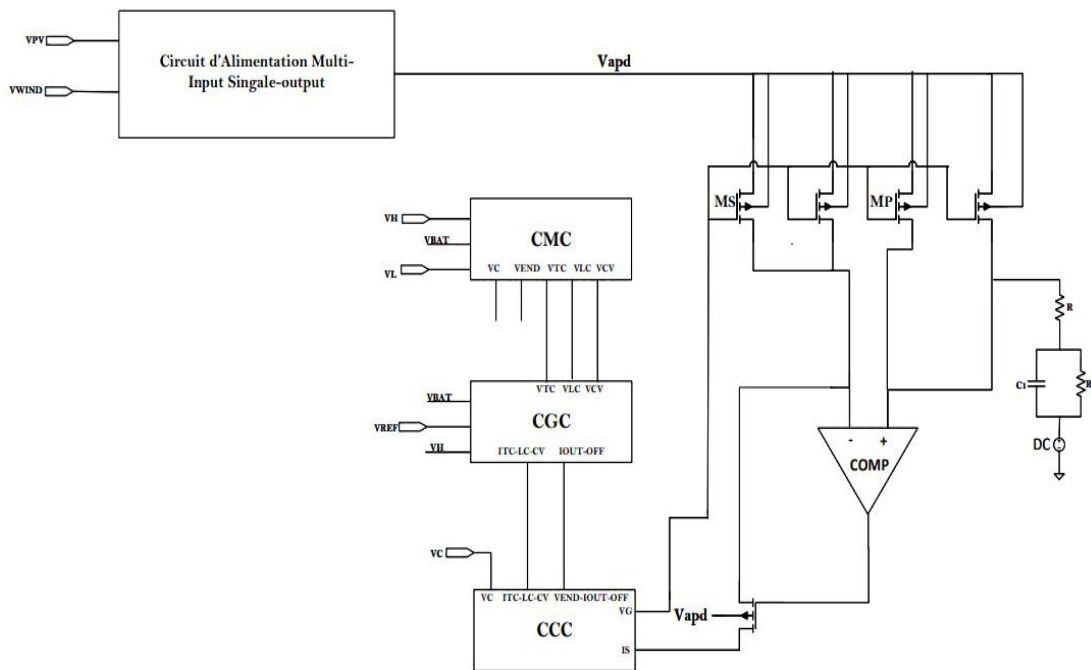
Figure 3. Proposed Lithium-Ion battery charger architecture

3.1. Power supply multi-input single-output circuit (the non-inverting summing)

The supply voltage is based on a non-inverting summing circuit. The main role of the summing circuit is to add the voltages V_{pv} and V_{wind} to obtain a voltage capable of charging the battery. This non-inverting summing unit consists of two operational amplifiers (OP) and resistors. Which depicted in Figure 4.

AOP is assumed to be ideal, in linear operation (V+=V-). Since the current I- is zero and the resistors are all equal to R1=R2=R3=R4=R5, we can write:

$$V^+ = V^- = 0 \qquad (3)$$

$$I_{pv} + I_{wind} = I \qquad (4)$$

$$\frac{V_{pv}}{R_1} + \frac{V_{wind}}{R_2} = -\frac{V_s}{R_3} \qquad (5)$$

when R1 = R2 = R3 = R4 = R5 = R then:

$$V_s = -(V_{pv} + V_{wind}) \qquad (6)$$

The output voltage Vs is therefore equal to the opposite of the sum of the different input voltages. As with differential amplifier 1, I don't see any immediate point in choosing different resistors to achieve this function. To invert the sign of Vs, an inverting amplifier with unity gain can be placed downstream, as shown in the Figure 4.
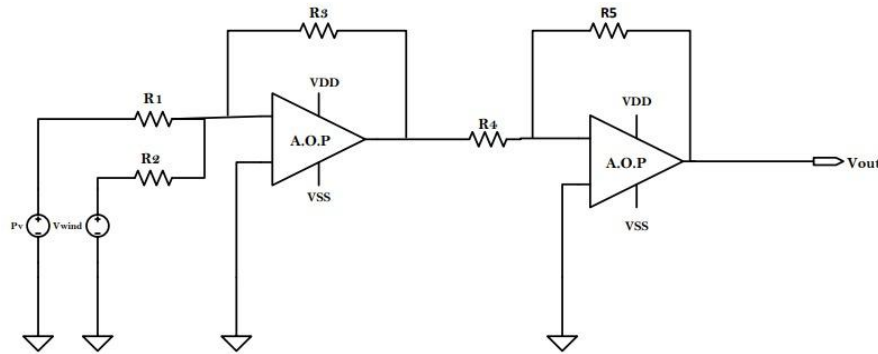
Figure 4. The non-inverting summing circuit

This is how the output voltage is expressed:

$$\frac{V_{out}}{V_s} = -\frac{R}{R} = -1 \qquad (7)$$

$$V_s = (V_{pv} + V_{wind}) \qquad (8)$$

3.2. The design and operating principle of the charge mode controller circuit

The logic circuit that powers the charging mode controller is made up of an inverter, NAND, OR, two analog comparators, and additional logic ports. The three V_{TC}, V_{LC}, and V_{CV} signals to control are produced by first comparing the battery voltage with the predefined reference voltage V_{Low}, V_{High} using a comparator. These signals primary function is to supply current through the RCG I_{TC}, I_{LC}, and I_{CV}, as seen in Figure 5. In every charging condition, the load current is provided by the control signal V_C.
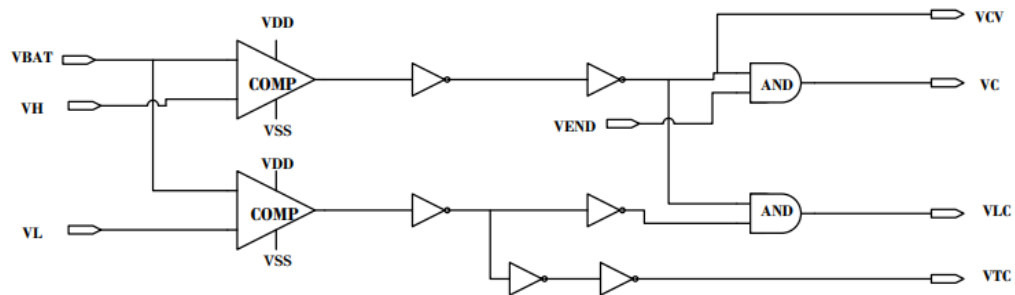
Figure 5. Charging mode controller

3.3. Circuit design and operating principal reference current generator

Figure 6 illustrates a RCG. It consists of a voltage unit and a current module. The OP amplifier acts as a voltage follower, the constant reference current I_{ref} is produced by transistor M_7 and resistor R_{REF}.

$$Iref = \frac{Vref}{R_{REF}} \tag{9}$$

The current mirror systems M_1, M_2, M_3 and finally IREF are proportional to the (10) to (12):

$$ITC = \frac{w_2/L_2}{w_1/L_1} Iref \tag{10}$$

$$ILC = \frac{w_3/L_3}{w_1/L_1} Iref \tag{11}$$

$$ICV = \frac{w_4/L_4}{w_1/L_1} Iref \tag{12}$$

Table 1 is function of the charge mode controller. In order to accomplish this, the voltage block's reference current for the CV load mode is created. The structure is made up of a comparator and the already-existing mirrors (M_5 and M_6). The following is the load current that the I_{CV} generates: when the battery voltage hits the 4.2V value, the comparator generates an I_{CV} current that changes from I_{LC} to I_{Off} High to Low level, as seen in Figure 6. As was previously noted, three transistors (M_{10}, M_9, and M_8) that are controlled by V_{TC}, V_{LC}, and V_{CV} in each charge mode provide a corresponding current for each charge mode.

Figure 6. Reference current generator circuit

Table 1. Function of the charge mode controller

Condition	V_{TC}	V_{LC}	V_{CV}	V_{END}	V_C
Constant trickle current	High	Low	Low	Low	High
Constant large current	Low	High	Low	Low	High
Constant voltage	Low	Low	High	Low	High
End of charging process	Low	Low	High	High	Low

3.4. The charging current controller circuit's design and operating principle

Figure 7 shows for every load mode, a control voltage VD from the current source is provided by the load current controller. The currents I_{TC}, I_{LC}, and I_{CV} from the RCG are compared with the current (*IS*) detected by the current sensor at the current comparator (transistors M_2–M_6). The (VD) output voltage is a function of these current inputs and is regarded as the selector high voltage level when the V_C is low and level as the lowest voltage level of the signal selector circuit, which consists of two transistors (M_1–M_4). At each load mode (low CC, high CC, and CV, current), the control voltage (VD) is finally established. The detected current (*IS*) and the reference current (ICut-off) are directly compared to initiate the end-of-charge mode operating independently.

The output voltage (VEND) of the current comparator (M_4 (RCG circuit), M_8) is at the lowest level when the detected current (*IS*) is larger than (ICut-off), allowing the regulated V_C to remain at the high level. In contrast, if the detected current (*IS*) is less than the input current (ICut-off), the gate drive signal (VD) is high, the current source is deactivated, along with the charge procedure is finished.
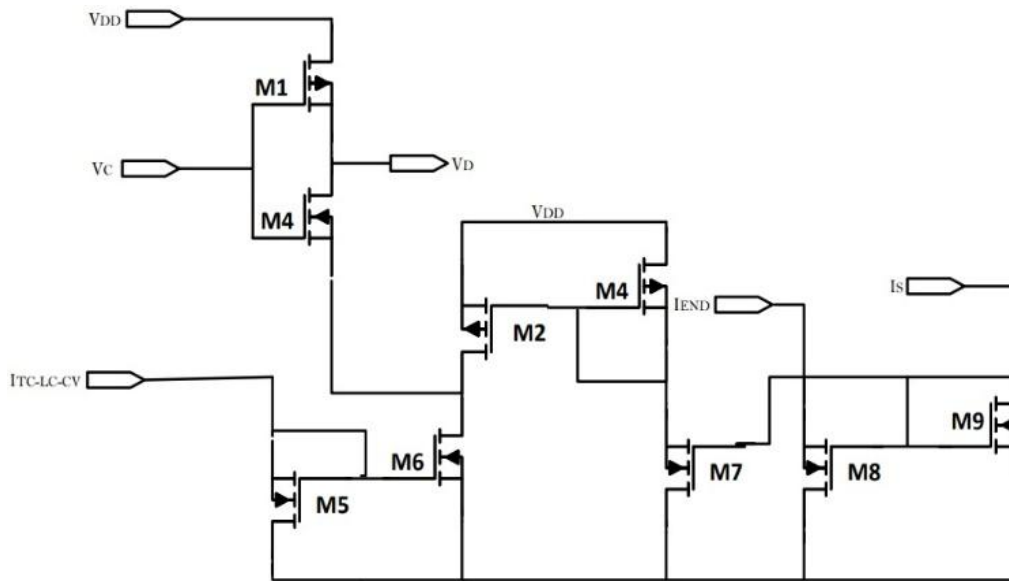
Figure 7. Charging current controller circuit

3.5. The circuit design and operating principle for the current source and current sensor

In the circuit illustrated in Figure 8, a MP power transistor is using as a variable current source to create a load current that corresponds to the I_{TC} in TC mode, I_{LC} during LC mode, a current I_{CV} degrading from the value of I_{LC} to the value of $Icut\text{-}off$ during CV mode and 0 A when the charging process is stopped. In addition, this PMOS MS transistor is used as a load current sensor. The following formulae can be used to characterize the currents of MP and Ms.

$$Is = \mu_P C_{ox} \left[{W_s}/{L_s} (V_{GS} - V_{TP})V_{SDS} - \frac{1}{2}V_{SDS}^2 \right] \tag{13}$$

$$Ich = \mu_P C_{ox} \left[{W_p}/{L_p} (V_{GS} - V_{TP})V_{SDP} - \frac{1}{2}V_{SDP}^2 \right] \tag{14}$$

The purpose of the OP is to maintain a constant drain voltage of Vd=Vb. Because of this, the load current flowing through power transistor MP is always equal to the current that transistor MS senses. In order that,

$$Ich = \frac{{w_p}/{L_p}}{{w_s}/{L_s}}.Is = NIs \tag{15}$$

where N is the number of transistor multiples.
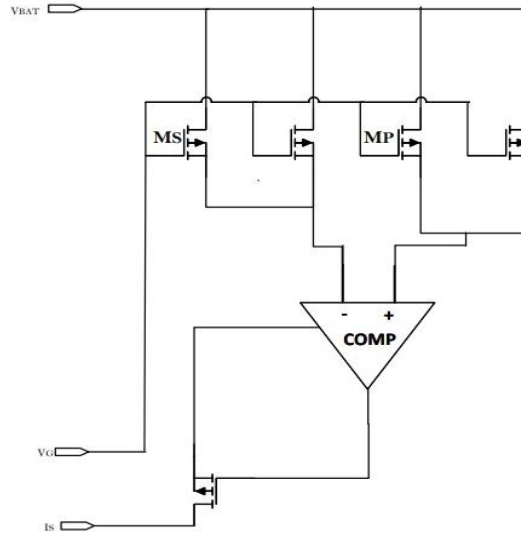
Figure 8. Circuit for the current sensor and current source

4.   RESULTS AND DISCUSSION

The proposed high-efficiency multi-source Lithium-Ion battery charger with multiple renewable energy sources has been simulated in Cadence Virtuoso using 180 nm CMOS technology. Figure 9 shows the simulation of a non-inverting voltage summator. The observed waveforms demonstrate the proper functioning of the circuit. The output voltage accurately represents the sum of the two input voltages, as expected from the design.
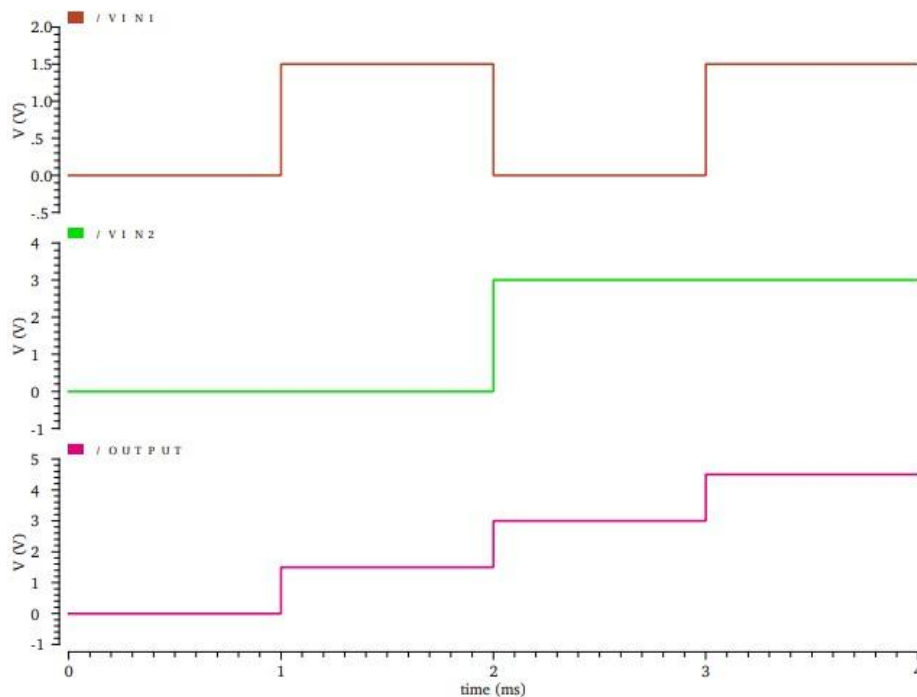
Figure 9. Non-inverting voltage summator circuit

The charge mode control circuit simulation results are shown in Figure 10. The figure illustrates the behavior of three charge mode control signals: V_{TC}, V_{LC}, and V_{CV}. Initially, V_{TC} drops quickly and then stabilizes, indicating a transition from a high-power phase to a controlled state. V_{LC} gradually increases to a

peak before decreasing and stabilizing, suggesting a ramp-up phase followed by stabilization. V_{CV} remains low initially, then sharply rises and returns to a stable state, indicating a voltage regulation phase. The coordinated changes and stability of these signals reflect an effective multi-stage charge control strategy, optimizing for efficiency and performance.

Figure 11 displays the findings of the analysis of the Lithuim-Ion battery charger suggested in this work. The battery voltage starts at approximately 2.75 V, steadily rising to about 4.25 V, indicating effective charging. Initially, the charge current surges to 1.5 A, maintaining this level until around 1.5 ks, before sharply decreasing to zero. This reflects a multi-phase charging process: a rapid charge phase, a CC phase, and a final CV phase to safely complete charging. The coordinated changes highlight an efficient strategy for balancing fast charging with battery safety.
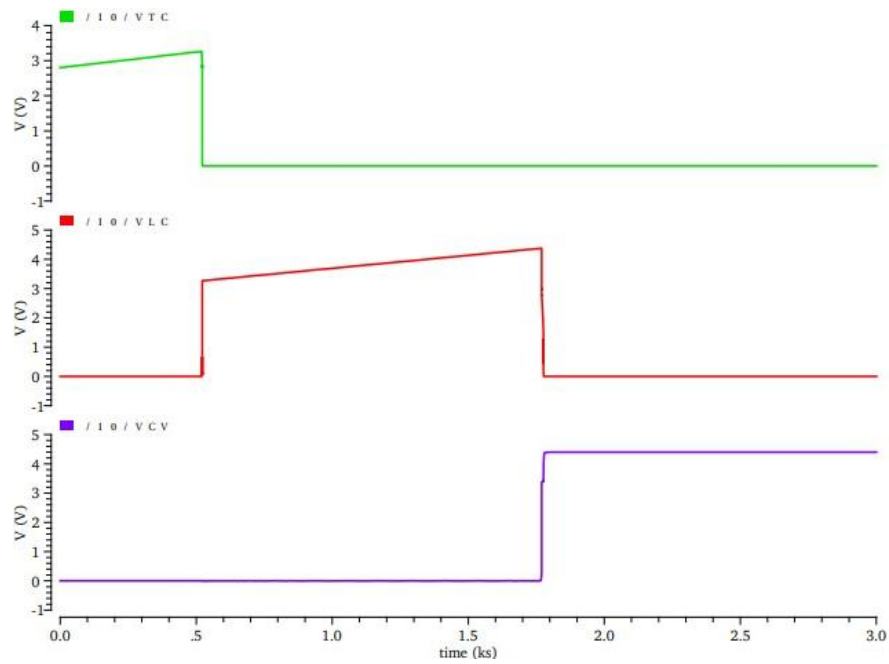
Figure 10. Charge mode control signals V_{TC}, V_{LC}, and V_{CV}
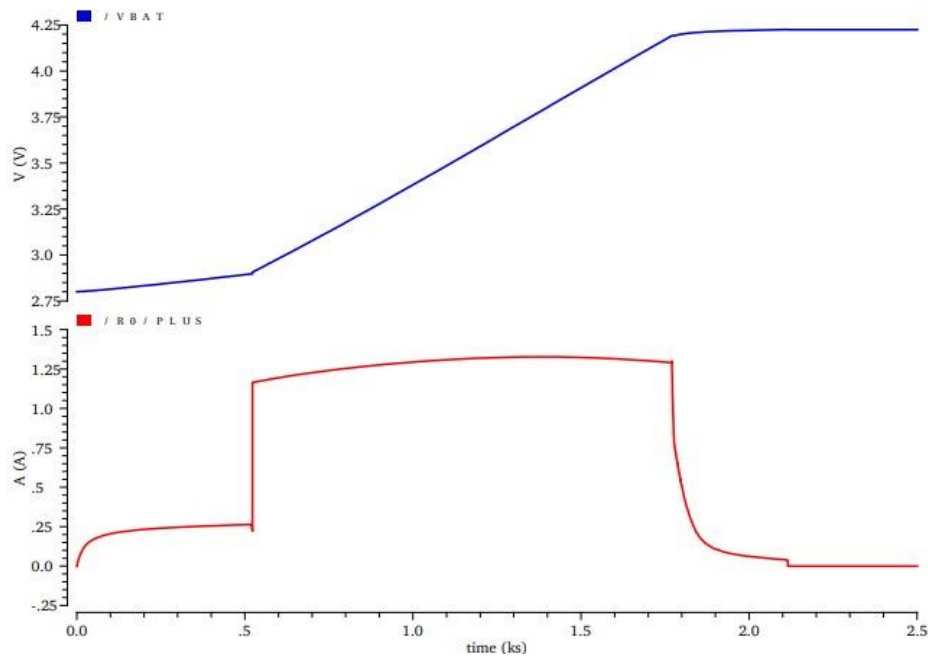
Figure 11. Charge current and battery voltage simulation results

High-efficiency multimode charging interface for Li-Ion battery with renewable … (Hajjar Mamouni)

Figure 12 shows the efficiency vs output current relationship of a device operating at a supply voltage of 4.5 V. The efficiency starts at around 88% and rises sharply, reaching a peak of over 92% around 1 A of output current. However, as the output current increases further, the efficiency gradually declines, dropping below 90% around 2 A and continuing to decrease as the current rises. A comparison between the proposed Li-Ion battery charger and other state-of-the-art chargers is summarized in Table 2.
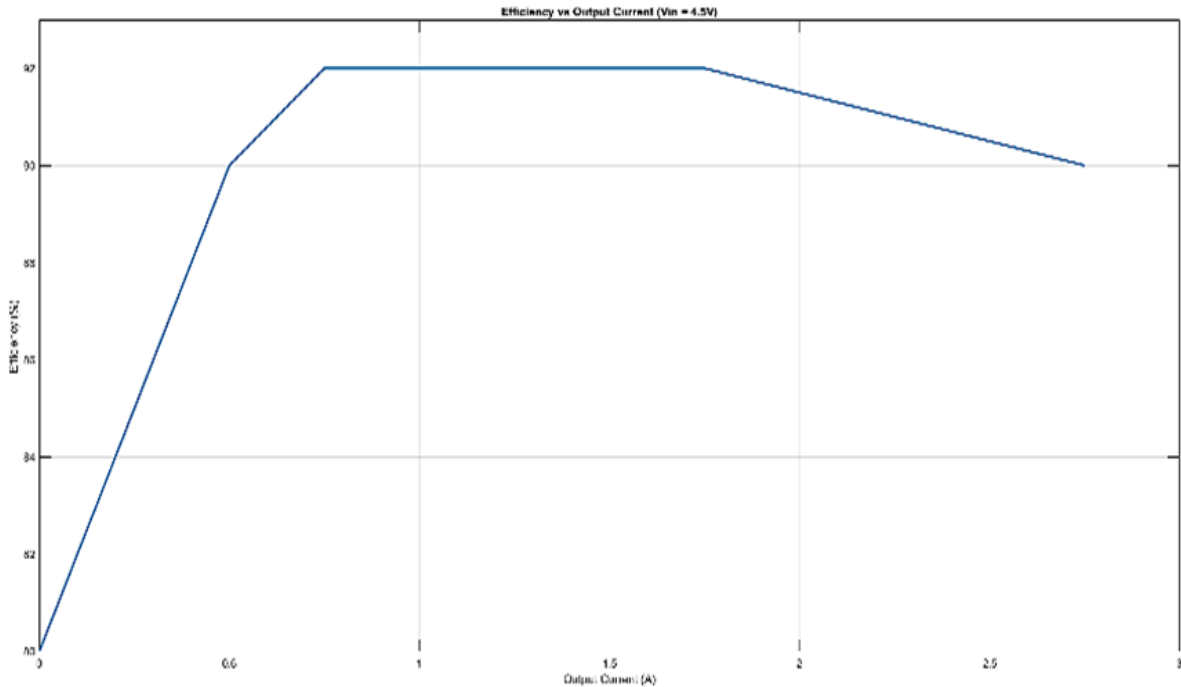
Figure 12. Efficiency vs output current simulation results

Table 2. Performance summary and comparison

Technology	Work by [22] CMOS 350 nm	Work by [6] CMOS 180 nm	Work by [23] CMOS 350 nm	Work by [24] CMOS 350 nm	Work by [25] CMOS 130 nm	This work CMOS 180 nm
Supply voltage	4.5 V	4.8-5 V	4.4 V	5.5 V	5 V	4.5 V
Efficiency (%)	70.09%	87%	80%	92%	83.9%	92%
Output voltage	4.2 V	4.2 V	4.1 V	4.2 V	4.3 V	4.2 V
Maximum charge current	700 mA	448 mA	1000 mA	600 mA	495 mA	1.3 A

5.   CONCLUSION

In conclusion, a new charging interface architecture with multimode control for a Li-Ion battery with multiple renewable energy sources in CMOS technology. The circuit design is capable of adapting to its environment and responding to a variety of applications. The proposed architecture optimizes energy transfer between sources and loads and improves system efficiency. The functions of the three stage charger include low CC charging (250 mA), high current charging (1.3 A) and CV charging (4.2 V). The Li-Ion battery charger offers a supply voltage of 4.5 V and the battery voltage is charged from 2.8 V to 4.2 V, it has a high energy efficiency equal to 92% and takes only 29 minutes to charge.

REFERENCES

[1]   M. Chen and G. A. Rincón-Mora, "Accurate, compact, and power-efficient Li-Ion battery charger circuit," *IEEE Transactions on Circuits and Systems II: Express Briefs*, vol. 53, no. 11, pp. 1180–1184, 2006, doi: 10.1109/TCSII.2006.883220.
[2]   H. Nguyen-Van, D. Nguyen, T. Nguyen, M. Nguyen, and L. Pham-Nguyen, "A Li-Ion battery charger with stable charging mode controller in noise environments," in *International Conference on Advanced Technologies for Communications*, 2016, pp. 270–274, doi: 10.1109/ATC.2015.7388333.
[3]   V. Teofilo, L. Merritt, and R. Hollandsworth, "Advanced Lithium-Ion battery charger," *IEEE Aerospace and Electronic Systems Magazine*, vol. 12, no. 11, pp. 30–36, 1997.

[4] Y. Ziadi and H. Qjidaa, "A high efficiency Li-Ion battery LDO-based charger for portable application," *Active and Passive Electronic Components*, pp. 1–9, 2015, doi: 10.1155/2015/591986.

[5] D. Linden and T. Reddy, "Handbook of batteries," in *Fuel and energy abstracts*, vol. 4, no. 36, New York, USA, 1995.

[6] M. Ouremchi *et al.*, "Li-Ion battery charger based on LDO regulator for portable device power management," 2018, doi: 10.1109/IRSEC.2018.8702961.

[7] K. El Khadiri, H. Akhmal, and H. Qjidaa, "Li-Ion battery charging with a buck-boost DC-DC converter for a portable device power management," *Journal of Low Power Electronics*, vol. 13, no. 2, pp. 263–270, 2017, doi: 10.1166/jolpe.2017.1479.

[8] T. T. K. Nga *et al.*, "A wide input range buck-boost DC-DC converter using hysteresis triple-mode control technique with peak efficiency of 94.8% for RF energy harvesting applications," *Energies*, vol. 11, no. 7, 2018, doi: 10.3390/en11071618.

[9] H. Wu, T. Mu, H. Ge, and Y. Xing, "Full-range soft-switching-isolated buck-boost converters with integrated interleaved boost converter and phase-shifted control," *IEEE Transactions on Power Electronics*, vol. 31, no. 2, pp. 987–999, 2016, doi: 10.1109/TPEL.2015.2425956.

[10] J. S. Kim, J. O. Yoon, J. Lee, and B. D. Choi, "High-efficiency peak-current-control non-inverting buck–boost converter using mode selection for single Ni–MH cell battery operation," *Analog Integrated Circuits and Signal Processing*, vol. 89, no. 2, pp. 297–306, 2016, doi: 10.1007/s10470-016-0787-0.

[11] Y.-Y. Tsai, Y.-S. Tsai, C.-W. Tsai, and C.-H. Tsai, "Digital noninverting-buck--boost converter with enhanced duty-cycle-overlap control," *IEEE Transactions on Circuits and Systems II: Express Briefs*, vol. 64, no. 1, pp. 41–45, 2016.

[12] S. Y. Cho, I. O. Lee, J. Il Baek, and G. W. Moon, "Battery impedance analysis considering dc component in sinusoidal ripple-current charging," *IEEE Transactions on Industrial Electronics*, vol. 63, no. 3, pp. 1561–1573, 2016, doi: 10.1109/TIE.2015.2497661.

[13] Z. Chen, B. Xia, C. C. Mi, and R. Xiong, "Loss-minimization-based charging strategy for Lithium-Ion battery," *IEEE Transactions on Industry Applications*, vol. 51, no. 5, pp. 4121–4129, 2015, doi: 10.1109/TIA.2015.2417118.

[14] Z. Guo, B. Y. Liaw, X. Qiu, L. Gao, and C. Zhang, "Optimal charging method for lithium ion batteries using a universal voltage protocol accommodating aging," *Journal of Power Sources*, vol. 274, pp. 957–964, 2015, doi: 10.1016/j.jpowsour.2014.10.185.

[15] S. Dearborn, "Charging Li-Ion batteries for maximum run times," *Power Electronics Technology*, vol. 31, no. 4, pp. 40–49, 2005.

[16] Y. S. Hwang, S. C. Wang, F. C. Yang, and J. J. Chen, "New compact CMOS Li-Ion battery charger using charge-pump technique for portable applications," *IEEE Transactions on Circuits and Systems I: Regular Papers*, vol. 54, no. 4, pp. 705–712, 2007, doi: 10.1109/TCSI.2007.890605.

[17] H. Y. Yang, T. H. Wu, J. J. Chen, Y. S. Hwang, and C. C. Yu, "An omnipotent Li-Ion battery charger with multimode controlled techniques," in *Proceedings of the International Conference on Power Electronics and Drive Systems*, 2013, pp. 531–534, doi: 10.1109/PEDS.2013.6527076.

[18] B. Do Valle, C. T. Wentz, and R. Sarpeshkar, "An area and power-efficient analog Li-Ion battery charger circuit," *IEEE Transactions on Biomedical Circuits and Systems*, vol. 5, no. 2, pp. 131–137, 2011, doi: 10.1109/TBCAS.2011.2106125.

[19] J.-J. Chen, F.-C. Yang, C.-C. Lai, Y.-S. Hwang, and R.-G. Lee, "A high efficiency multimode Li-Ion battery charger with variable current source and controlling previous-stage supply voltage," *IEEE transactions on industrial electronics*, vol. 56, no. 7, pp. 2469–2478, 2009.

[20] L. Pengfei, R. Bashirullah, and J. C. Principe, "A low power battery management system for rechargeable wireless implantable electronics," in *Proceedings - IEEE International Symposium on Circuits and Systems*, 2006, pp. 1139–1142, doi: 10.1109/iscas.2006.1692791.

[21] H. Nguyen-Van, T. Nguyen, V. Quan, M. Nguyen, and L. Pham-Nguyen, "A topology of charging mode control circuit suitable for long-life Li-Ion battery charger," in *2016 IEEE 6th International Conference on Communications and Electronics, IEEE ICCE 2016*, 2016, pp. 167–171, doi: 10.1109/CCE.2016.7562630.

[22] H. M. Nguyen, L. D. Pham, and T. Hoang, "A novel Li-Ion battery charger using multi-mode LDO configuration based on 350 nm HV-CMOS," *Analog Integrated Circuits and Signal Processing*, vol. 88, no. 3, pp. 505–516, 2016, doi: 10.1007/s10470-016-0778-1.

[23] J. A. De Lima, "A compact and power-efficient CMOS battery charger for implantable devices," 2014, doi: 10.1145/2660540.2660988.

[24] C. C. Su, Y. W. Liu, and C. C. Hung, "A dual-input high-efficiency Li-Ion battery charger with current-mode smooth transition and ripple reduction circuits," *Midwest Symposium on Circuits and Systems*, pp. 468–471, 2017, doi: 10.1109/MWSCAS.2017.8052961.

[25] K. Chung, S. K. Hong, and O. K. Kwon, "A fast and compact charger for an Li-Ion battery using successive built-in resistance detection," *IEEE Transactions on Circuits and Systems II: Express Briefs*, vol. 64, no. 2, pp. 161–165, 2017, doi: 10.1109/TCSII.2016.2554839.

BIOGRAPHIES OF AUTHORS

Hajjar Mamouni 🔴 SC ↻ in 2022, he obtained a Master's degree in Microelectronics from the Faculty of Sciences at Dhar El Mahraz in Fez, Morocco. Currently, she is a Ph.D. student at the LISAC Laboratory in the Department of Physics at Sidi Mohammed Ben Abdellah University, Fez, Morocco. She can be contacted at email: hajar.mamouni@usmba.ac.ma.

Karim El Khadiri 🆔 📷 sc ◐ is now a Professor in Superior Normal School, ENS-FEZ, Morocco. He received his Master degree since 2011 in Micro-Electronics and Ph.D. degrees since 2017 in FSDM, USMBA, Fez, Morocco. His research interests include Li-Ion battery charger interface (BCI) and BMS, RFID passive and active tags, CMOS mixed mode integrated circuit design, Integrated Class-D power output stage and renewable energy. He can be contacted at email: karim.elkhadiri@usmba.ac.ma.

Anass El Affar 🆔 📷 sc ◐ is now a Professor in Department of computer science, FP Taza, USMBA, Fez, Morocco. He received his master's degree since 2003 and Ph.D. degrees since 2009 in computer science from FSDM, USMBA, Fez, Morocco. His research interests include BIG DATA, renewable energy, machine learning and image processing. He can be contacted at email: anass.elaffar@usmba.ac.ma.

Mohammed Ouazzani Jamil 🆔 📷 sc ◐ is currently a Professor in Private university of Fez (UPF). He does research in Condensed Matter Physics, Hamiltonian system, chaos, renewable energy and artificial intelligence. Their current project is dynamic systems. He can be contacted at email: ouazzani@upf.ac.ma.

Hassan Qjidaa 🆔 📷 sc ◐ is now a Professor in Department of Physics, FSDM, USMBA, Fez, Morocco. He received his master's degree since 1984 and Ph.D. degrees since 1987 in Electrical Engineering from Nuclear Physics Institute of Lyon, France. His research interests include Li-Ion ba tery charger interface (BCI) and BMS, RFID passive and active tags, CMOS mixed mode integrated circuit design, Integrated Class-D power output stage, renewable energy, and image processing. He can be contacted at email: hassan.qjidaa@usmba.ac.ma.